

Electronic Supplementary Information (ESI†)

**Resorcinol-formaldehyde semiconducting resins as precursors  
for carbon spheres toward electrocatalytic oxygen reduction**

Yasuhiro Shiraishi,\* Keisuke Kinoshita, Keisuke Sakamoto, Koki Yoshida, Wataru Hiramatsu,  
Satoshi Ichikawa, Shunsuke Tanaka, and Takayuki Hirai

shiraishi.yasuhiro.es@osaka-u.ac.jp

**CONTENTS**

	Page
<b>Methods</b> .....	2
<b>Table S1</b> Elemental composition of the samples.....	4
<b>Fig. S1</b> SEM images .....	5
<b>Fig. S2</b> DLS results.....	6
<b>Fig. S3</b> N <sub>2</sub> adsorption/desorption data .....	7
<b>Fig. S4</b> Powder XRD patterns .....	8
<b>Fig. S5</b> Survey XPS spectra.....	9
<b>Fig. S6</b> XPS (C1s) results.....	10
<b>Fig. S7</b> XPS (N1s) results.....	11
<b>Fig. S8</b> Raman spectra .....	12
<b>Fig. S9</b> STEM-EDS observation results of RF-523_NH <sub>3</sub> .....	13
<b>Fig. S10</b> STEM-EDS observation results of RF-523_Ar .....	14
<b>References</b> .....	15

## Methods

### Materials

Water was purified by the Milli-Q system. Resorcinol, formaldehyde (37 wt% solution), NH<sub>3</sub> (28 wt% solution), and other chemicals were purchased from Wako. Nafion (5 wt%) dispersion solution was purchased from Sigma-Aldrich. The Pt/C catalyst (Pt 10 wt%, TEC10E10E) was purchased from Tanaka Precious Metals. They were used without further purification.

### Synthesis of RF-*x*\_resins

The RF-*x*\_resin powders (*x* = 373, 473, and 523 K) were prepared as follows:<sup>[1]</sup> resorcinol (800 mg, 7.2 mmol), formaldehyde (33 wt% solution, 1.08 mL, 14.4 mmol) and NH<sub>3</sub> (28 wt% solution, 360 μL, 6.0 mmol) were added to water (80 mL). The mixture (pH 8.8) was stirred for 10 min at room temperature. The white colloidal suspension was transferred to a Teflon-lined stainless-steel autoclave and left in an oven at the designated temperatures (*x* K) for 12 h. The solids formed were washed thoroughly by Soxhlet extraction using acetone for 12 h and dried in vacuo at room temperature, affording RF-*x*\_resin powders.

### Synthesis of RF-*x*\_Ar or RF-*x*\_NH<sub>3</sub>

The RF-*x*\_Ar or RF-*x*\_NH<sub>3</sub> were prepared by pyrolysis of RF-*x*\_resin under Ar gas flow (50 mL min<sup>-1</sup>) or 10% NH<sub>3</sub>/He mixed gas flow (50 mL min<sup>-1</sup>) in a tubular furnace at 1173 K, with a heating rate of 12.5 K min<sup>-1</sup> and a holding time of 2 h, respectively.

### LSV measurements

All potential values were normalized to the reversible hydrogen electrode (RHE) scale using the following equation.<sup>[2]</sup>

$$\begin{aligned} E(\text{vs. RHE}) &= E(\text{vs. Ag/AgCl}) + E(\text{Ag/AgCl (ref)}) + 0.0591\text{V} \times \text{pH}(= 13.0) \\ &= E(\text{vs. Ag/AgCl}) + 0.9659\text{ V} \end{aligned}$$

The LSV measurements were performed at room temperature in a RRDE system (RRDE-3A, BAS) using 0.1 M KOH (pH 13.0, 80 mL) as an electrolyte. The counter and reference electrodes were Pt coil and Ag/AgCl, respectively, and the working RRDE electrode consists of a glassy carbon disk (φ4.0 mm) and a Pt ring (φ5.0 mm). The catalyst powder (4.1 mg) was dispersed in a mixture of ethanol (1680 μL), water (420 μL), and a Nafion 5 wt% dispersion (30 μL). The suspension was ultrasonicated for 1 min, 8 μL of the dispersion was put onto a glassy carbon disk, and the electrode was dried at room temperature. The amount of the catalyst loaded was 123 μg cm<sup>-2</sup>. All LSV measurements were performed after O<sub>2</sub> bubbling through the electrolyte for 10 min. The current was monitored at between 0.15 V and -0.8 V (vs. Ag/AgCl) with a scan rate of 2 mV s<sup>-1</sup> and a rotating speed of 1600 rpm. During the measurements, the ring potential was maintained at 0.15 V (vs. Ag/AgCl). The electron transfer number (*n*<sub>ET</sub>) for ORR on the electrode was determined using the following equation:

$$n_{\text{ET}} = \frac{4 \times I_{\text{D}}}{I_{\text{D}} + I_{\text{R}}/N}$$

$I_{\text{D}}$  is disk current,  $I_{\text{R}}$  is ring current, and  $N$  is the collection efficiency of the ring ( $N = 0.424$ ) determined by the sizes of disk and ring electrodes.<sup>[3]</sup>

### EIS measurements

The EIS measurements were performed in 0.1 M Na<sub>2</sub>SO<sub>4</sub> or 0.1 M KOH (50 mL) electrolytes using a three-electrode cell.<sup>[4]</sup> The counter and reference electrodes were a Pt coil and Ag/AgCl, respectively. The working electrodes were prepared using a fluorine tin oxide (FTO) glass (2 cm<sup>2</sup>). Catalyst (20 mg) was mixed with water (2 mL), 2-propanol (750 μL), and a 5 wt% Nafion dispersion (50 μL). The suspension was ultrasonicated for 1 min. The slurry (100 μL) was put onto a FTO glass and dried at room temperature. The catalyst area was shaped as 0.5 cm square (0.25 cm<sup>2</sup>). The measurements were performed at a bias of -0.4 V (vs. Ag/AgCl) and a frequency range from 1 Hz to 10 kHz.

### Analysis

SEM observations were performed using a S-5000H FE-SEM (Hitachi High-Tech). DLS analysis was performed using ELSZ-2000S analyzer (Otsuka Electronics).<sup>[5]</sup> XPS spectra were measured on a JPS-9010MX (JEOL) spectrometer with an Mg-K $\alpha$  radiation. The N<sub>2</sub> adsorption/desorption measurements were performed at 77 K using a BELSORP MINI X (Microtrac BEL).<sup>[6]</sup> The specific surface areas and pore size distributions were determined on the basis of the Brunauer–Emmett–Teller (BET) and Barrett–Joyner–Halenda (BJH) methods, respectively. Powder XRD patterns were recorded on the X'Pert PRO MPD (PANalytical) X-ray diffractometer with Cu-K $\alpha$  radiation. Raman spectra was recorded on a LabRAM HR-800 (Horiba) with a 532 nm excitation laser.<sup>[7]</sup> STEM–EDS observations were conducted on a JEOL JEM-ARM200F microscope at 200 kV.<sup>[8]</sup>

**Table S1** Elemental compositions of the samples determined by the combustion method.

	C / wt%	O / wt% <sup>[a]</sup>	N / wt%	H / wt%
RF-373 resin	56.73	36.91	1.18	5.18
RF-523 resin	67.37	26.74	0.64	5.25
RF-373_Ar	95.09	3.99	0.67	0.25 <sup>[b]</sup>
RF-523_Ar	95.84	4.02	0.14	0
RF-373_NH <sub>3</sub>	83.16	8.80	7.50	0.84 <sup>[b]</sup>
RF-523_NH <sub>3</sub>	86.16	6.29	7.01	0.54 <sup>[b]</sup>

[a] Determined using the following equation:

$$\text{O (wt \%)} = 100 - [\text{C (wt \%)} + \text{N (wt \%)} + \text{H (wt \%)}]$$

[b] The H component may be attributable to the adsorbed water.

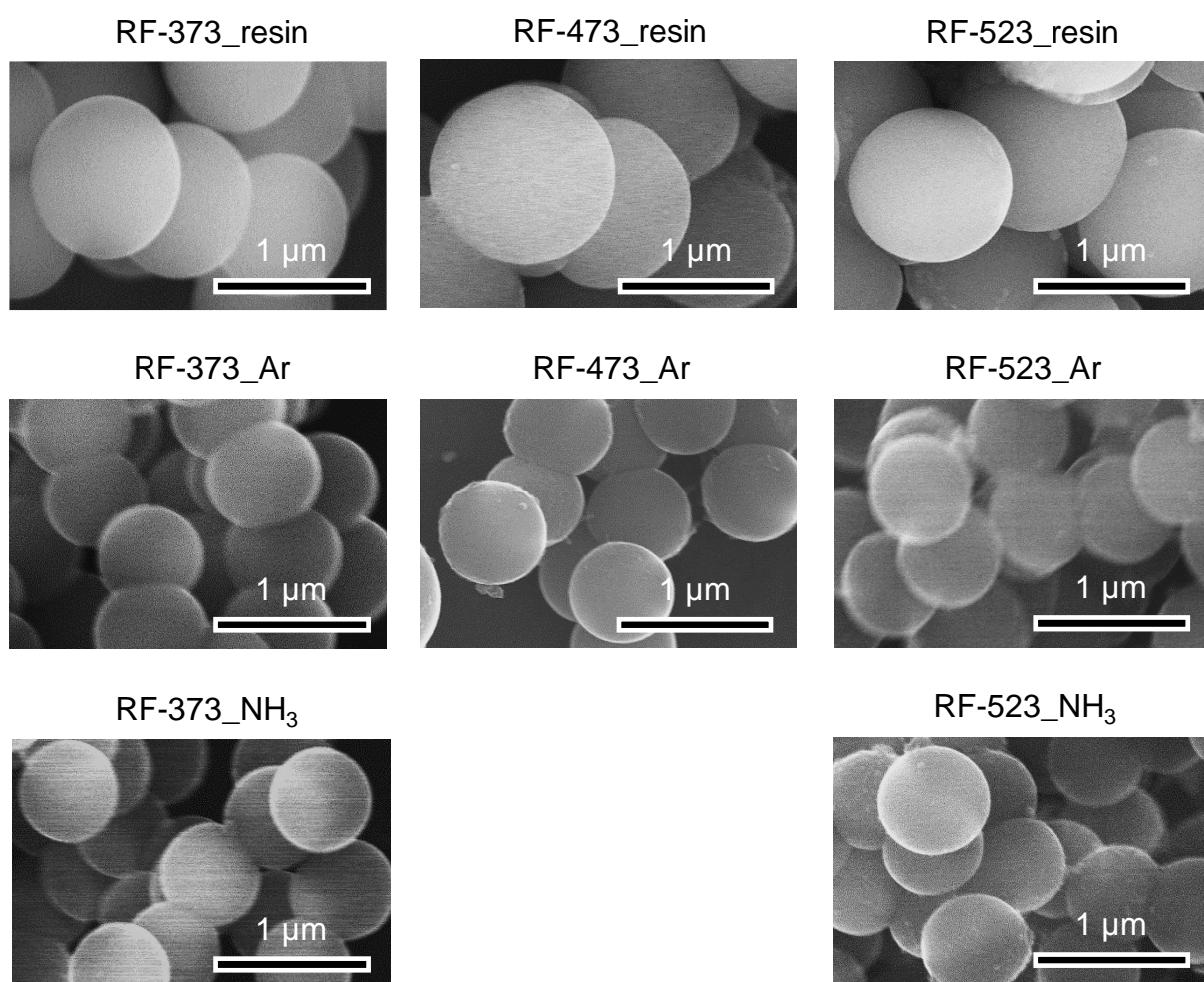


**Fig. S1** SEM images of RF-*x*\_resins, RF-*x*\_Ar, and RF-*x*\_NH<sub>3</sub>.

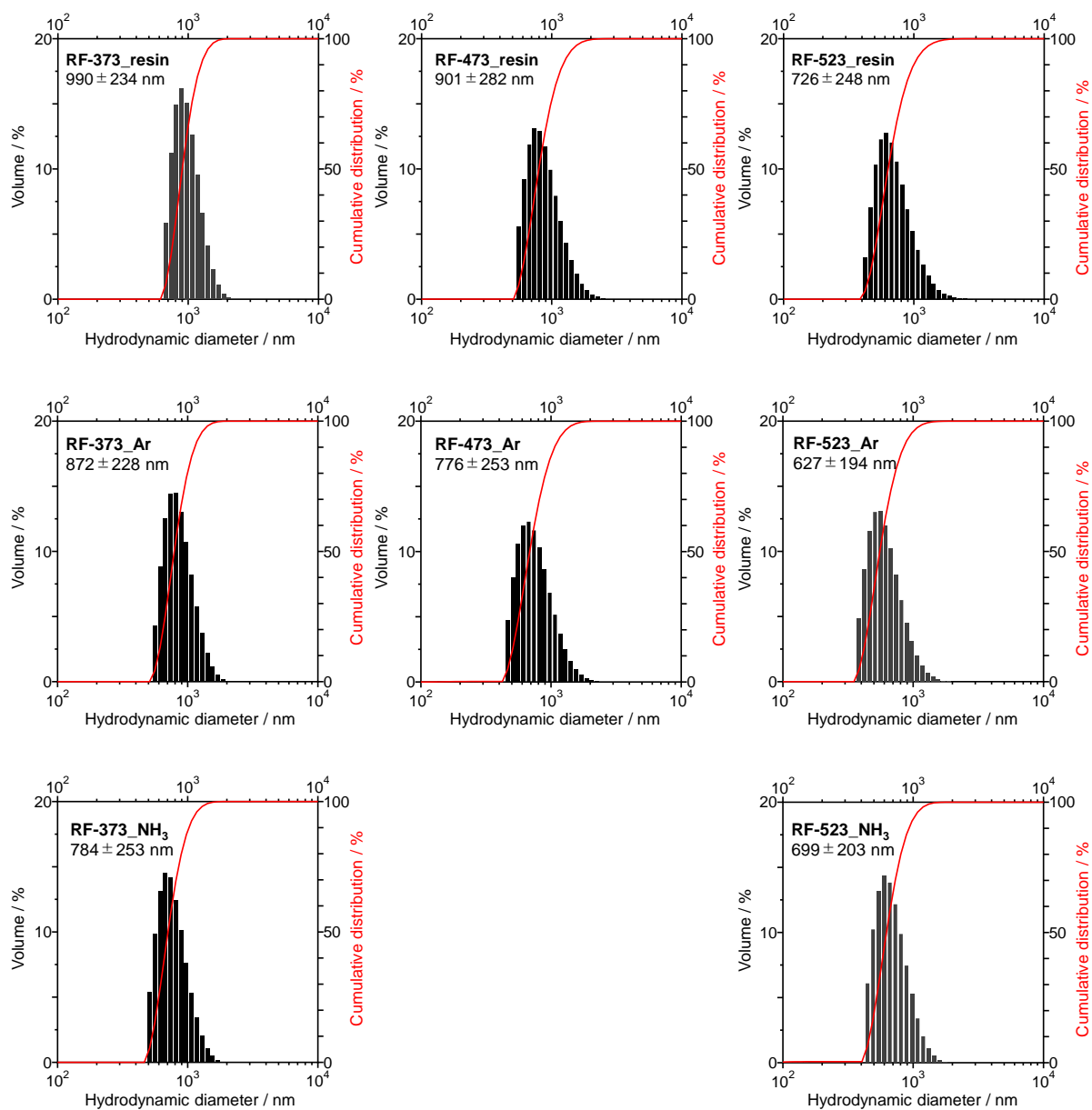


**Fig. S2** DLS results of RF-*x*\_resins, RF-*x*\_Ar, and RF-*x*\_NH<sub>3</sub>.

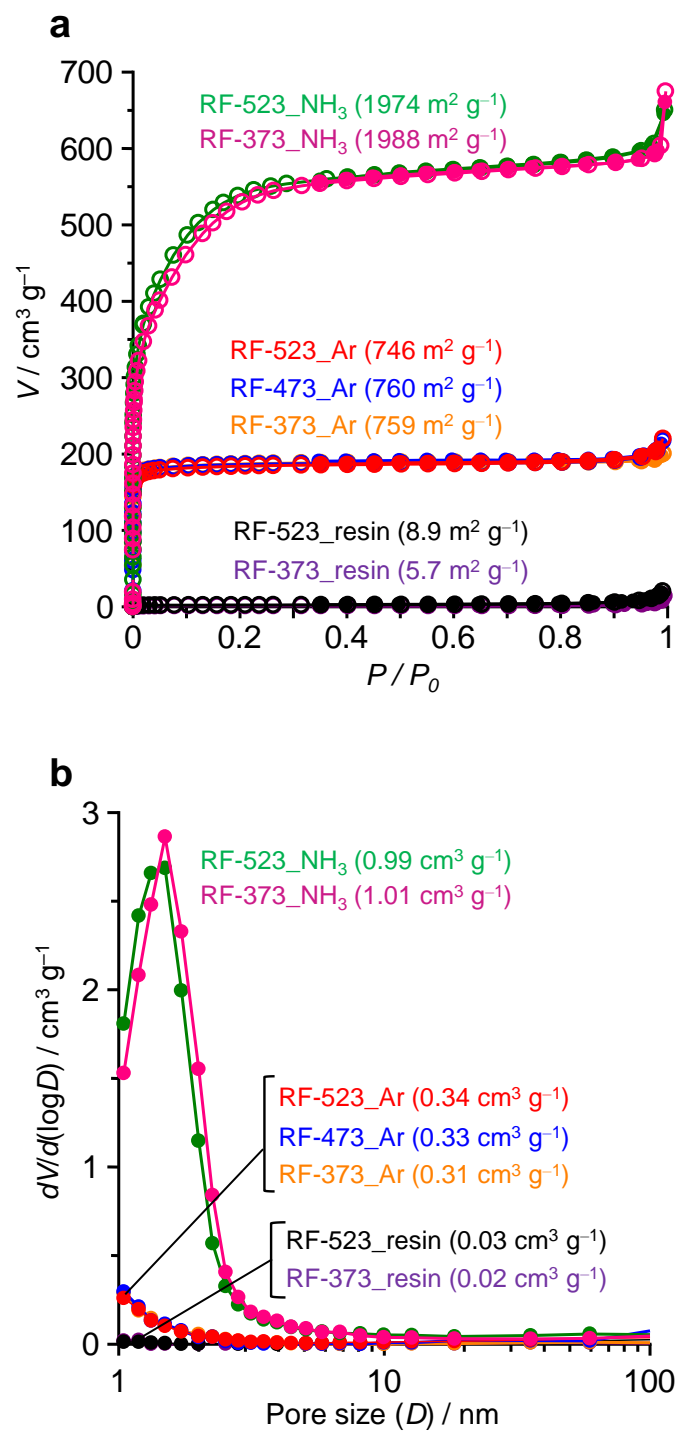


**Fig. S3** (a) N<sub>2</sub> adsorption/desorption isotherms and (b) corresponding pore size distributions of RF-*x*\_resins, RF-*x*\_Ar, and RF-*x*\_NH<sub>3</sub>.

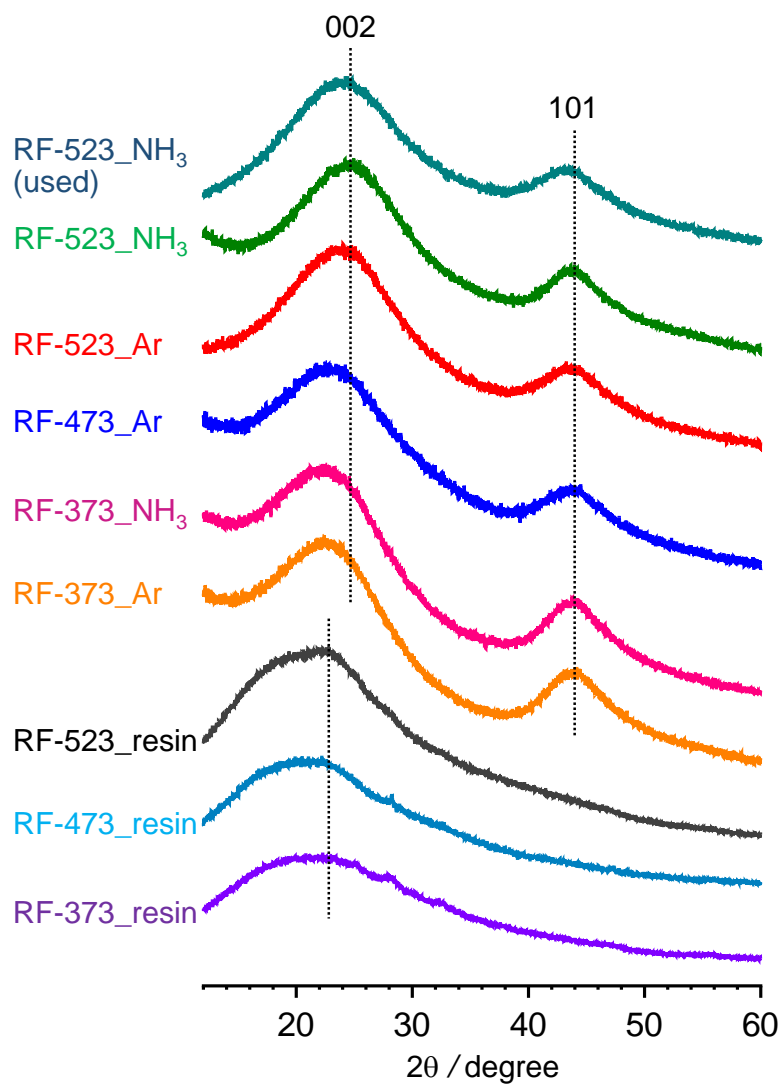


**Fig. S4** Powder XRD patterns of fresh RF-*x*\_resins, RF-*x*\_Ar, RF-*x*\_NH<sub>3</sub>, and the recovered RF-523\_NH<sub>3</sub> after CV cycles (Fig. 4a).



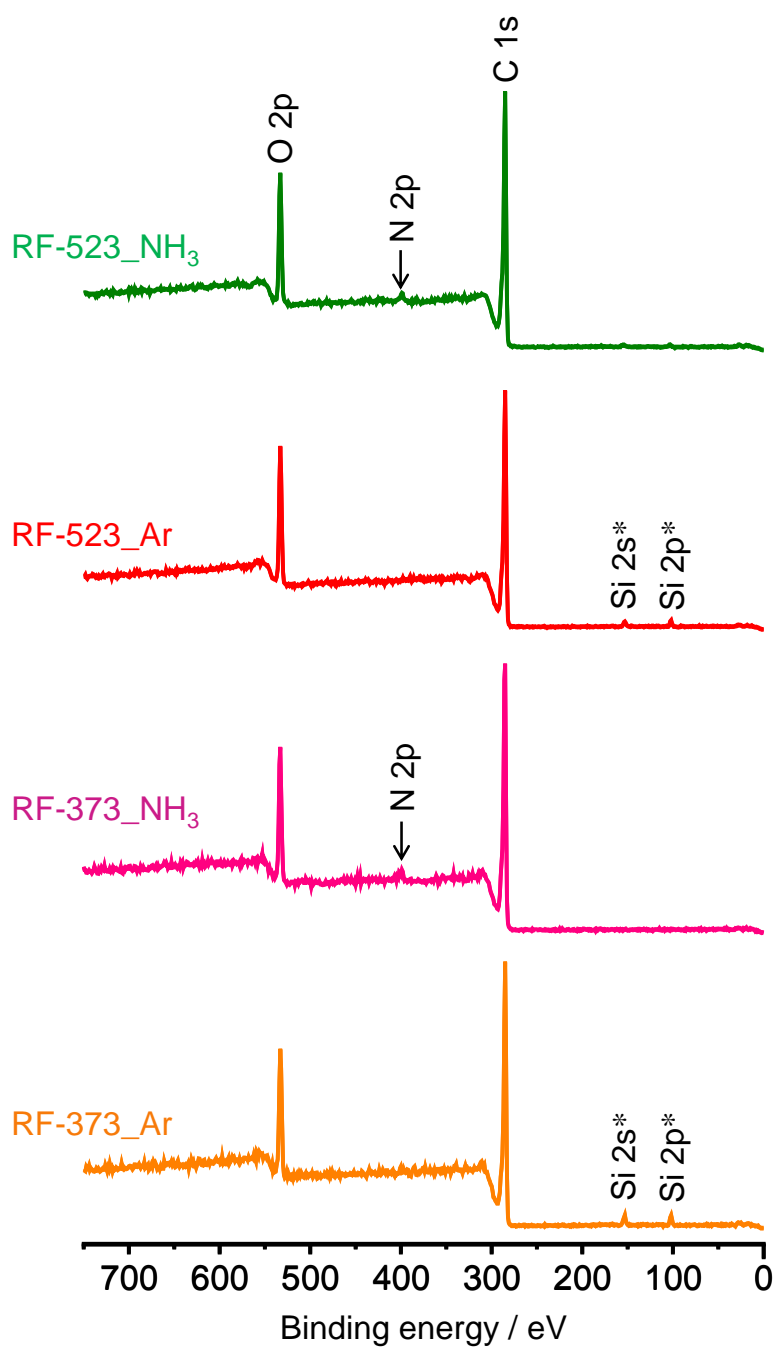


**Fig. S5** Survey XPS spectra of RF- $x$ \_Ar and RF- $x$ \_NH<sub>3</sub>. The asterisks denote the impurities of the sample grid.

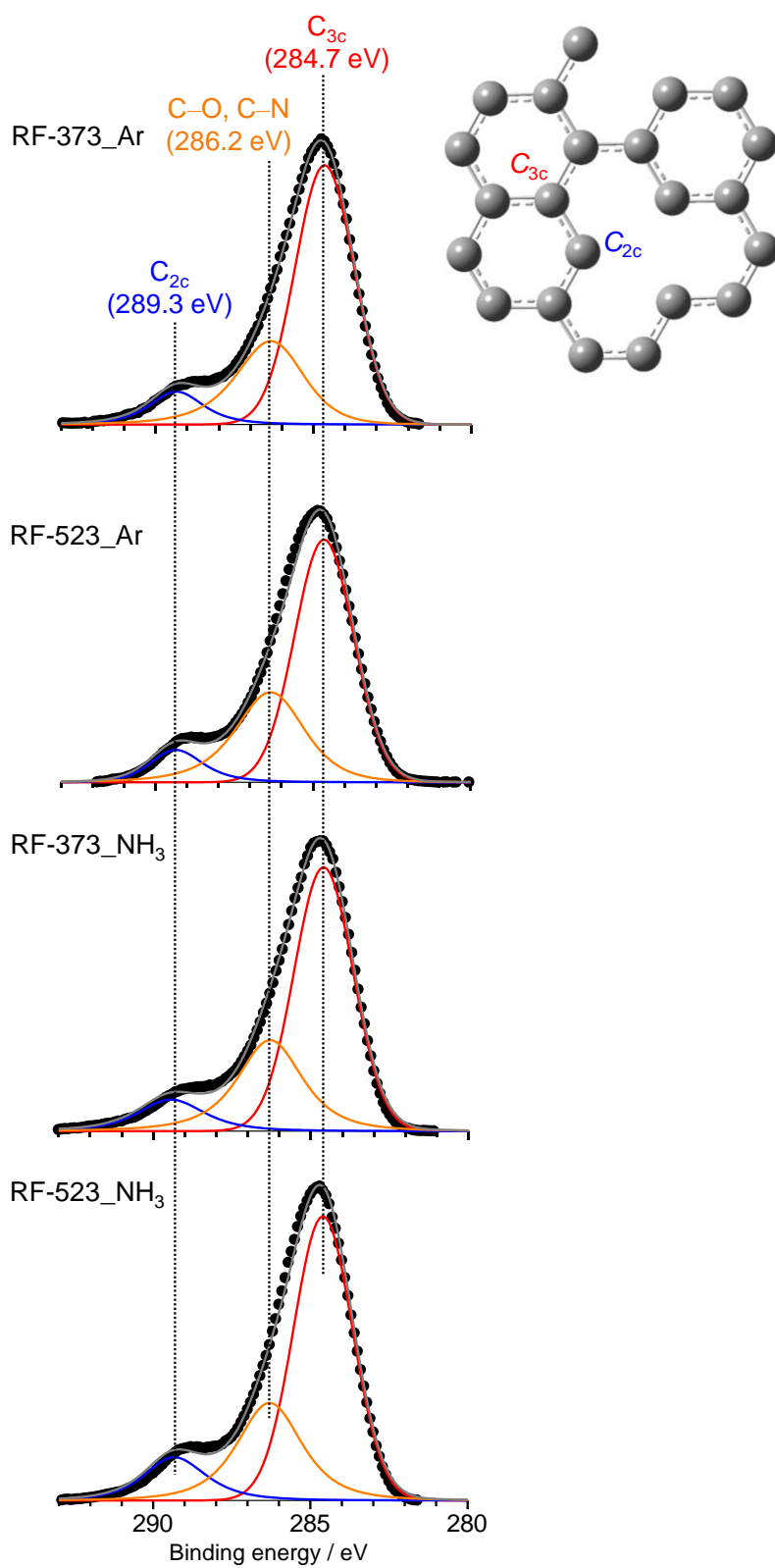


**Fig. S6** C 1s XPS of RF- $x$ \_Ar and RF- $x$ \_NH<sub>3</sub>.

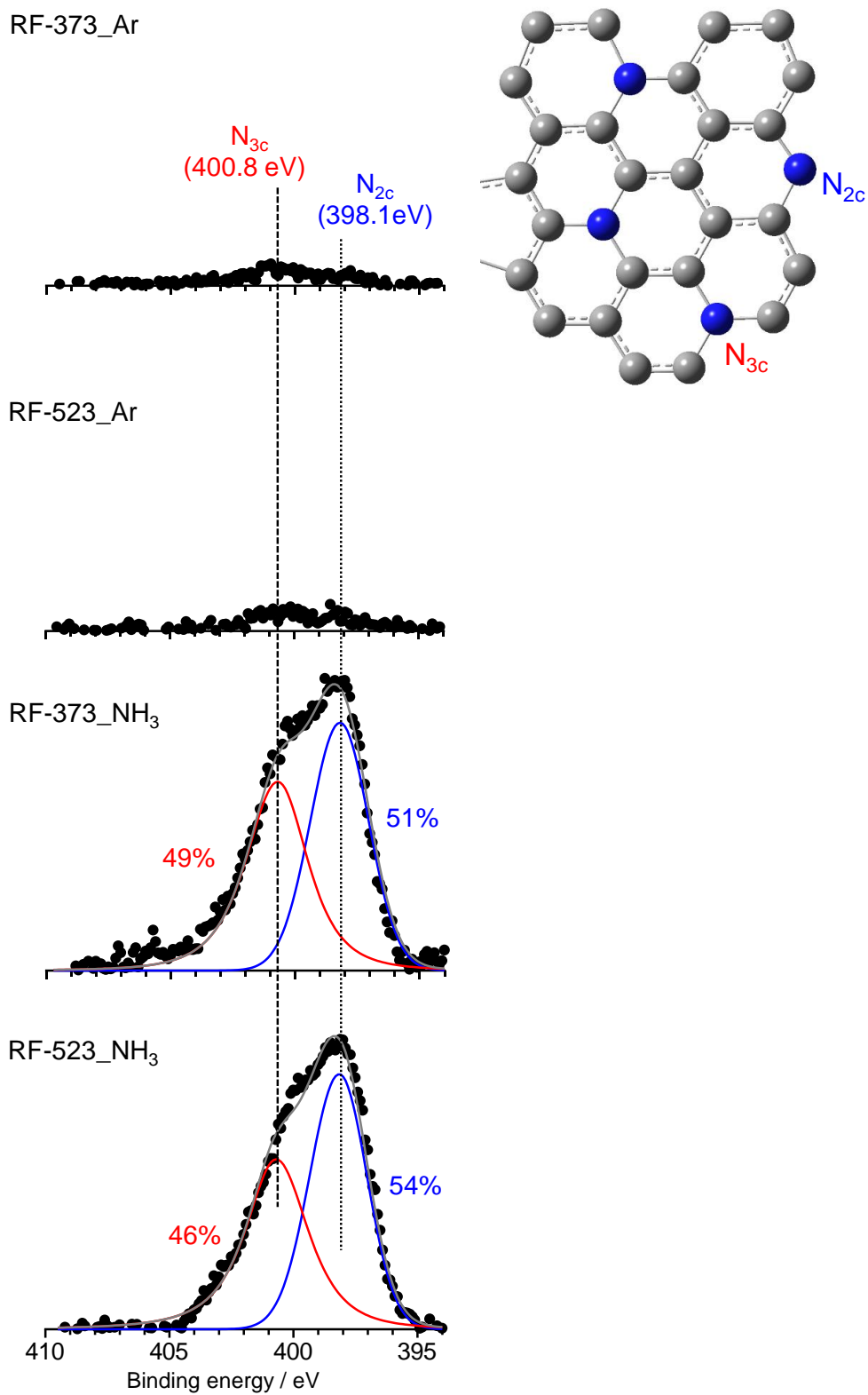
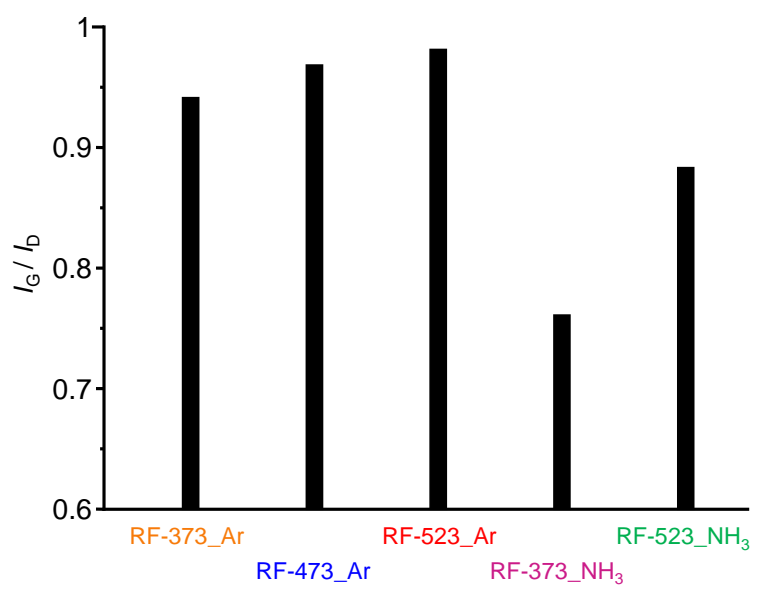
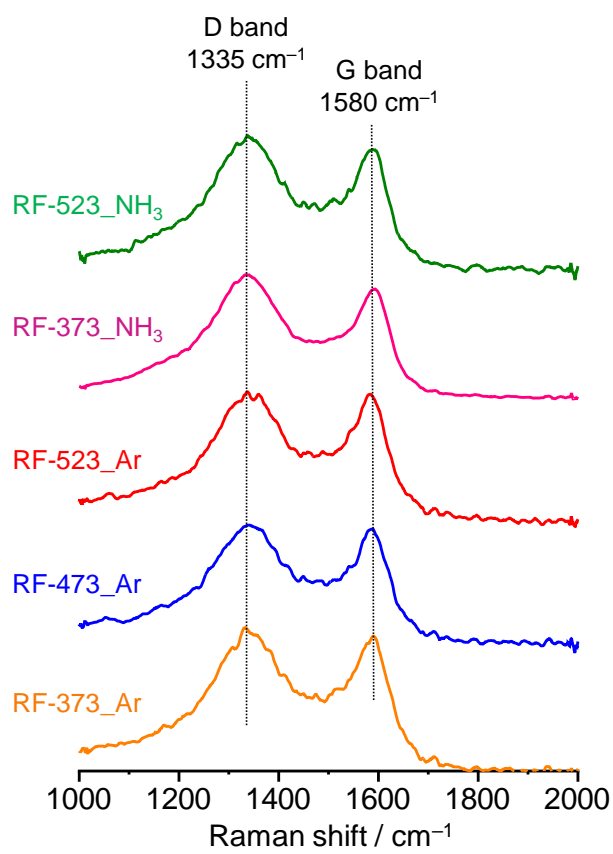
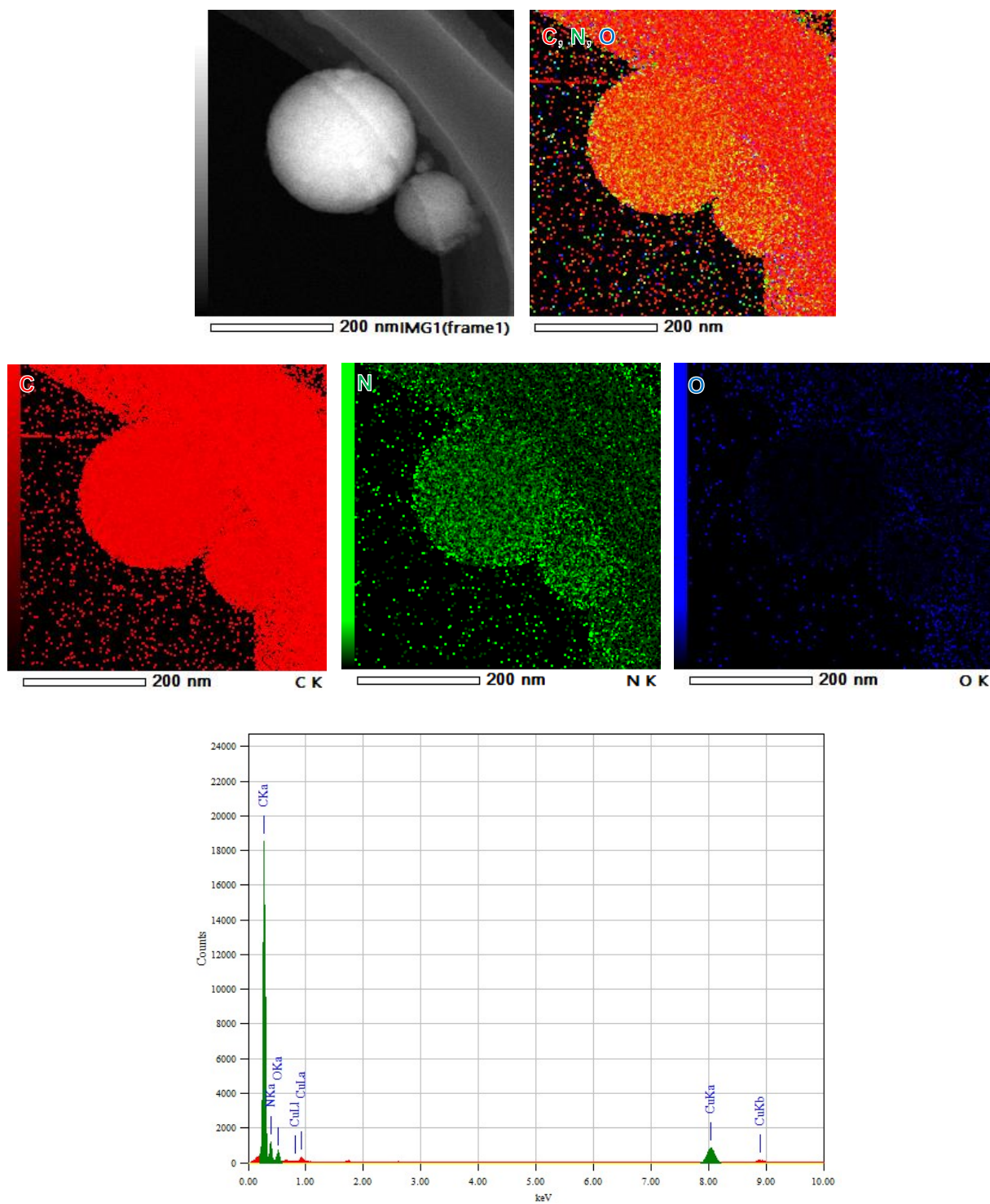


Fig. S7 N 1s XPS of RF- $x$ \_Ar and RF- $x$ \_NH<sub>3</sub>.



**Fig. S8** Raman spectra of RF-*x*\_Ar and RF-*x*\_NH<sub>3</sub>, and the corresponding  $I_G/I_D$  data.



**Fig. S9** STEM images, EDS quantitative maps, and EDS spectrum of RF-523\_NH<sub>3</sub> spheres. The EDS maps (K $\alpha$  line) consist of C (red), N (green), and O (blue) components.

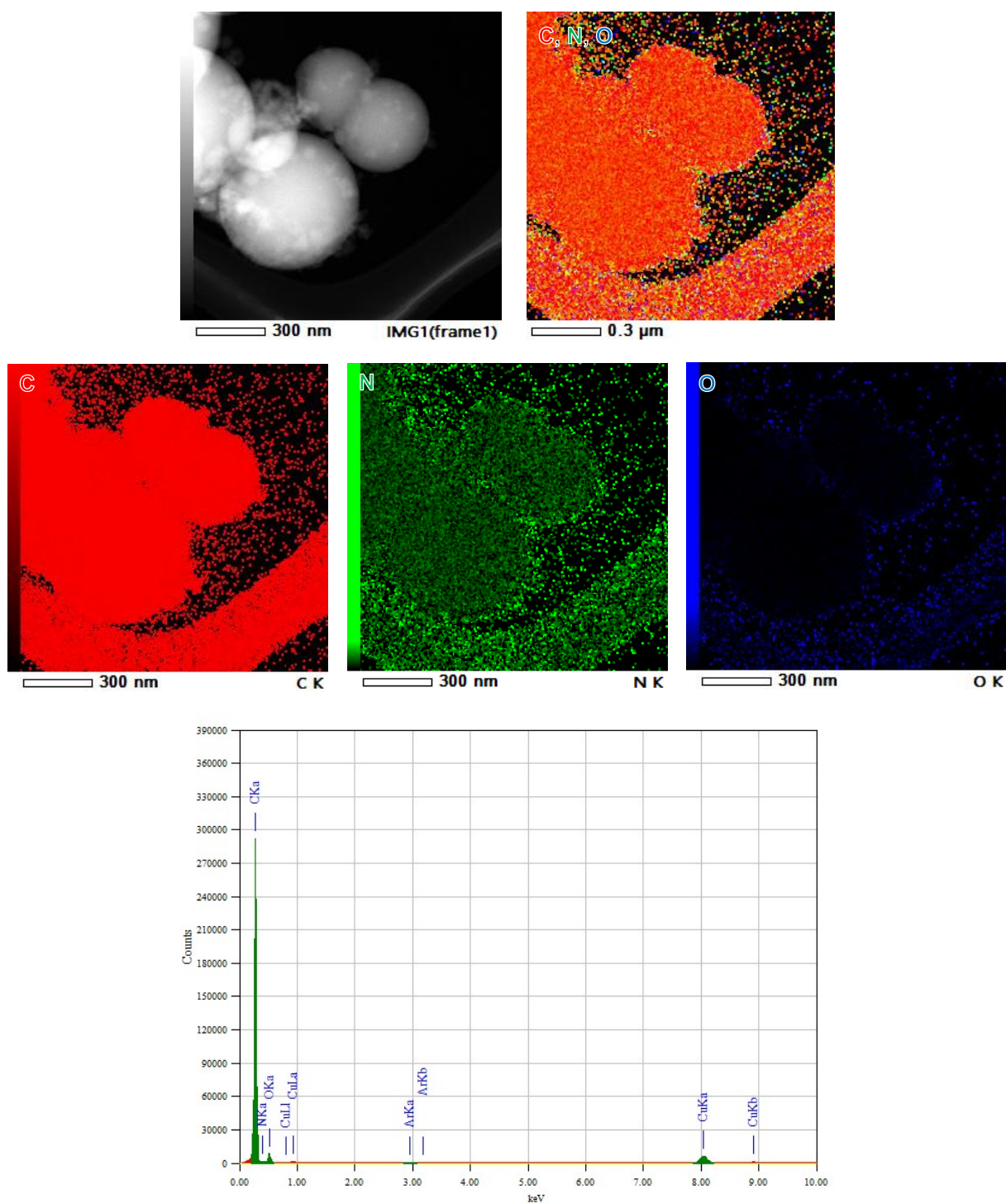


**Fig. S10** STEM images, EDS quantitative maps, and EDS spectrum of RF-523\_Ar spheres. The EDS maps ( $K\alpha$  line) consist of C (red), N (green), and O (blue) components.

## References

- [1] Y. Shiraishi, T. Takii, T. Hagi, S. Mori, Y. Kofuji, Y. Kitagawa, S. Tanaka, S. Ichikawa and T. Hirai, *Nat. Mater.*, 2019, **18**, 985.
- [2] J. A. Seabold and K. S. Choi, *J Am. Chem. Soc.*, 2012, **134**, 2186.
- [3] K. Gong, F. Du, Z. Xia, M. Durstock and L. Dai, *Science*, 2009, **323**, 760.
- [4] Y. Shiraishi, Y. Shimabukuro, K. Shima, S. Ichikawa, S. Tanaka and T. Hirai, *JACS Au*, 2023, **3**, 1403.
- [5] Y. Shiraishi, M. Jio, K. Yoshida, Y. Nishiyama, S. Ichikawa, S. Tanaka and T. Hirai, *JACS Au*, 2023, **3**, 2237.
- [6] Y. Shiraishi, S. Akiyama, W. Hiramatsu, K. Adachi, S. Ichikawa and T. Hirai, *JACS Au*, 2024, **4**, 1863.
- [7] Y. Shiraishi, Y. Ueda, A. Soramoto, S. Hinokuma and T. Hirai, *Nat. Commun.*, 2020, **11**, 3386.
- [8] Y. Shiraishi, M. Matsumoto, S. Ichikawa, S. Tanaka and T. Hirai, *J. Am. Chem. Soc.* 2021, **143**, 12590.